FORWARD COMPTON SCATTERING[†]

Marc Damashek[*] and Frederick J. Gilman

Stanford Linear Accelerator Center, Stanford University, Stanford, California

ABSTRACT

An analysis of the recently measured photon-proton total cross sections is performed. Smooth fits to the cross sections are obtained and used to calculate, by means of the forward dispersion relation, the real part of the spin-averaged forward amplitude. The resulting predictions for the real part are given. At high energies the fits to the present total cross section data together with the calculated real part suggest the presence in the high energy behavior of an extra real constant in addition to what one would have predicted from Regge theory and the high energy behavior of the imaginary part. This extra real constant, which is consistent in sign and magnitude with the Thomson limit, $-\alpha/M_N$, could correspond to a fixed pole at $J=0$ in Regge pole language. Possible ways to test the forward dispersion relation are discussed.

I. INTRODUCTION

In the fifteen years that have passed since the introduction of dispersion relations into elementary particle physics, originally within the context of quantum field theory, a large literature has grown up on their theoretical basis, on extensions and applications to new processes, and on their comparison with experiment. While first proposed for the amplitudes in forward Compton scattering by Gell-Mann, Goldberger, and Thirring[1], dispersion relations were soon written down and proved, with varying degrees of rigor, for forward pion-nucleon scattering, other forward amplitudes, various off-shell amplitudes and vertex functions, and for non-forward amplitudes[2]. These integral relations between the dispersive and absorptive parts of the scattering amplitude have been most thoroughly tested experimentally in the case of forward pion-nucleon scattering. Starting with the work of Anderson et al.[3] in the resonance region and proceeding through the recent high energy measurements of the real part of the forward amplitude and its comparison with the predictions of the forward dispersion relations by Foley et al.[4], the pion-nucleon dispersion relations have been subjected to extensive testing by comparison with both low and high energy experiments.

While all these tests in strong interactions have been successful, somewhat surprisingly the first such relations to be written down, those for forward Compton scattering, are still essentially untested. First, this is because the imaginary part of the forward Compton amplitude, in the form of total photoabsorption cross sections, has not been systematically measured until this past year. Previously, one only had the results of integrating the

single pion photoproduction differential cross sections over all angles to obtain

the total cross section near threshold and in the first resonance region (say,

up to 1.300 GeV center of mass energy) and some scattered bubble chamber

measurements at higher energies. Second, the real part of the forward ampli-

tude for Compton scattering was, and still is, unmeasured in both magnitude

and sign.

Within the past year this situation has changed rather dramatically.

We now have good systematic measurements of the unpolarized total photo-

absorption cross section (and therefore the imaginary part of the spin-averaged

forward Compton amplitude) from threshold up to laboratory photon energies

of almost 20 GeV. This permits one to calculate rather accurately the real

part of the spin-averaged forward amplitude using the dispersion relation

originally proposed by Gell-Mann, Goldberger, and Thirring[1]. The result of this

calculation can be compared in magnitude with forthcoming measurements at SLAC

of the forward Compton scattering differential cross section. Furthermore, it

now appears possible that by observing the interference between the known

Bethe-Heitler amplitude for producing electron-positron pairs and the Compton

contribution to pair production, both the sign and magnitude of the real part of

the Compton amplitude may be determined[5].

With all this in mind we have done a careful analysis of, and fit to,

the total photoabsorption cross section measurements, and have calculated

the real part of the forward Compton amplitude, both to look for places and

ways to test the forward dispersion relation and to investigate certain questions

of theoretical interest concerning the asymptotic behavior of the real part. In

Section II we discuss kinematics, the definition of the relevant amplitudes,

and the corresponding dispersion relations. We follow this with an analysis

of, and fits to, the total photoabsorption cross sections at low and high energies

in Section III, in preparation for the actual calculation of the real part of the

spin-averaged forward amplitude in Section IV using the dispersion relation.

The results of this calculation lead us to a discussion of the probable existence

in the high energy behavior of the forward amplitude of an extra real constant

part in addition to what one would have predicted from Regge theory and the

behavior of the imaginary part. This could be due to a fixed pole at $J = 0$ in

Regge language; such a real constant part is detectable both by a direct cal-

culation of the real part of the amplitude using the dispersion relation, and by

certain sum rules discussed in Section V. Finally, conclusions and suggestions

for further experimental measurements are given in Section VI.

II. THE FORWARD COMPTON AMPLITUDES

If the S-matrix element for the process $\gamma(k_1) + N(p_1) \rightarrow \gamma(k_2) + N(p_2)$ is

written as

$$S_{fi} = \delta_{fi} + (2\pi)^4 i \delta^{(4)}(p_2 + k_2 - p_1 - k_1) \sqrt{\frac{M_N^2}{4k_{10}k_{20}E_1E_2}} \; \bar{u}(p_2) \, T \, u(p_1) \; , \qquad (1)$$

where k_1 and p_1 (k_2 and p_2) are the four-momenta of the initial (final) photon

and nucleon, respectively, then the differential cross section in the center of

mass frame is given by

$$\frac{d\sigma}{d\Omega_{cm}} = |f^{cm}|^2 \qquad (2)$$

with the center of mass scattering amplitude, f^{cm}, being

$$f^{cm} = \frac{M_N}{4\pi W} \, \bar{u}(p_2) \, Tu(p_1) \; . \qquad (3)$$

Here W is the total center of mass energy; $W^2 = (p_1 + k_1)^2 = (p_2 + k_2)^2$. If we specialize to the case of forward scattering, then there is only one remaining continuous variable on which the scattering depends. We take this to be W as defined above, or instead of W, we will often use the energy of the photon in the laboratory, ν, which is related to W by

$$\nu = \frac{W^2 - M_N^2}{2M_N}.$$
(4)

It will, in fact, generally be convenient to work in terms of laboratory quantities. To this end we define the forward scattering amplitude in the laboratory, $f(\nu)$, which is related to the center of mass amplitude by a simple factor of W/M_N:

$$f(\nu) = \frac{W}{M_N} f^{cm}.$$
(5)

Written out between the Pauli spinors of the initial and final nucleons, which are at rest in the laboratory, $f(\nu)$ must have the form[1]

$$f(\nu) = \chi_f^* \left[f_1(\nu) \, \vec{\epsilon}_2^{\,*} \cdot \vec{\epsilon}_1 + i\vec{\sigma} \cdot (\vec{\epsilon}_2^{\,*} \times \vec{\epsilon}_1) f_2(\nu) \right] \chi_i$$
(6)

where ϵ_1 and ϵ_2 are the polarization vectors of the initial and final photons, respectively. Clearly, if we average over nucleon spins in the amplitude we are left only with $f_1(\nu)$ which we therefore call the spin-averaged forward amplitude. The amplitudes $f_1(\nu)$ and $f_2(\nu)$ are separable if we are able to do experiments with polarized photons: $f_1(\nu)$ corresponds to parallel and $f_2(\nu)$ to perpendicular linear polarization vectors of the initial and final photons respectively.

Another way of discussing the relationship between f_1 and f_2 is to relate them to the two independent helicity amplitudes for forward scattering. If the photon and proton spins are parallel (i.e., photon helicity $= +1$, nucleon helicity $= -\frac{1}{2}$ in the center of mass frame) then we have

$$f_p(\nu) = \frac{W}{M_N} f^{cm}_{1-\frac{1}{2},\,1-\frac{1}{2}}(\nu) = f_1(\nu) - f_2(\nu) ; \qquad (7a)$$

while if the spins are anti-parallel (i.e., photon helicity $= +1$, nucleon helicity $= +\frac{1}{2}$ in the center of mass) we have

$$f_a(\nu) = \frac{W}{M_N} f^{cm}_{1\frac{1}{2},\,1\frac{1}{2}}(\nu) = f_1(\nu) + f_2(\nu) . \qquad (7b)$$

It is the amplitudes f_p and f_a which are then related simply by the optical theorem to the total cross sections for photon + nucleon $\rightarrow$ hadrons (we shall work only to order e^2 in the amplitude) when the photon spin is parallel or anti-parallel to the nucleon spin:

$$\text{Im} f_p(\nu) = \frac{\nu}{4\pi} \sigma_p(\nu) \qquad (8a)$$

$$\text{Im} f_a(\nu) = \frac{\nu}{4\pi} \sigma_a(\nu) . \qquad (8b)$$

Thus we have

$$\text{Im} f_1(\nu) = \frac{\nu}{4\pi} \frac{\sigma_a(\nu) + \sigma_p(\nu)}{2} = \frac{\nu}{4\pi} \sigma_T(\nu) , \qquad (9a)$$

where $\sigma_T(\nu)$ is the spin-averaged total cross section, and

$$\text{Im} f_2(\nu) = \frac{\nu}{4\pi} \frac{\sigma_a(\nu) - \sigma_p(\nu)}{2} . \qquad (9b)$$

Again, in the absence of <u>both</u> a <u>circularly</u> polarized photon beam and a polarized

proton target, it is only the combination of cross sections corresponding to

$\text{Im} f_1(\nu)$ which is measured experimentally. Note also that while $\text{Im} f_p$, $\text{Im} f_a$,

and therefore $\text{Im} f_1$ are positive above threshold for pion photoproduction, $\text{Im} f_2$

may be either positive or negative there.

In the absence of polarized targets or beams one simply measures

the differential cross section

$$\left(\frac{d\sigma}{d\Omega_{\text{lab}}}\right)_{\theta=0^\circ} = |f(\nu)|^2 = |f_1(\nu)|^2 + |f_2|^2 \tag{10a}$$

or

$$\frac{d\sigma}{dt}\Big|_{t=0} = \frac{\pi}{\nu^2}|f(\nu)|^2 = \frac{\left[\sigma_T(\nu)\right]^2}{16\pi} + \frac{\pi}{\nu^2}|\text{Re} f_1(\nu)|^2 + \frac{\pi}{\nu^2}|f_2(\nu)|^2 \tag{10b}$$

where t is minus the square of the four-momentum transfer. We have explicitly

isolated the term proportional to $\left[\sigma_T(\nu)\right]^2$, which has now been systema-

tically measured experimentally, to emphasize the remaining terms on the right

hand side of Eq. (10b), which are uncalculated and unmeasured up to now.

If we know their imaginary parts, we may calculate $\text{Re} f_1(\nu)$ and

$\text{Re} f_2(\nu)$ by means of dispersion relations. Using the fact that $f_1(\nu)$ is even and

$f_2(\nu)$ is odd under crossing (i.e., $\nu \to -\nu$) we have[1]

$$\text{Re} f_1(\nu) = f_1(0) + \frac{\nu^2}{\pi} P \int_{\nu_0}^{\infty} \frac{d\nu'^2}{\nu'^2 - \nu^2} \frac{\text{Im} f_1(\nu')}{\nu'^2} , \tag{11a}$$

and

$$\text{Re} f_2(\nu) = \frac{2\nu}{\pi} P \int_{\nu_0}^{\infty} \frac{d\nu'}{\nu'^2 - \nu^2} \text{Im} f_2(\nu') . \tag{11b}$$

Both integrals start at $\nu_0 = m_\pi + m_\pi^2/2M_N$, the threshold for photoproducing single pions. In hopes that we can get away without a subtraction, and since we know of no experimental or theoretical reason for one, we have written an unsubtracted dispersion relation for $f_2(\nu)$. The amplitude $f_1(\nu)$ on the other hand requires a subtraction, both because of the observed behavior of $\mathrm{Im}\, f_1(\nu)$ for large ν and because an unsubtracted dispersion relation for $f_1(\nu)$ would predict $f_1(0) > 0$, contradicting the Thomson limit, $f_1(0) = -\alpha/M_N$. We in fact know from rather general theorems[6,7] that as $\nu \to 0$

$$f_1(\nu) \to f_1(0) = -\alpha/M_N \ , \tag{12a}$$

the Thomson limit, while

$$f_2(\nu)/\nu \to f_2'(0) = -\frac{\alpha(\mu_{anom})^2}{2M_N^2} \ . \tag{12b}$$

The second result, Eq. (12b), together with the dispersion relation (11b) gives rise to the sum rule

$$(\mu_{anom})^2 = -\frac{4M_N^2}{\pi\alpha} \int_{\nu_0}^{\infty} \frac{d\nu'}{\nu'^2} \,\mathrm{Im}\, f_2(\nu') = \frac{M_N^2}{2\pi^2\alpha} \int_{\nu_0}^{\infty} \frac{d\nu'}{\nu'} \left[\sigma_p(\nu) - \sigma_a(\nu)\right] . \tag{13}$$

This is just the Drell-Hearn-Gerasimov sum rule[8], which appears to be satisfied when saturated with low lying resonances[9]. Unfortunately, the lack of direct experimental measurements of $\mathrm{Im}\, f_2(\nu)$ means that one must construct it from partial wave analyses of πN (and if one is brave enough, $\pi\Delta$) photo-production[8,9]. While this is probably adequate for calculating $f_2'(0)$, the

difficulties and ambiguities in this procedure even in the resonance region presently make evaluation of the dispersion relation for $f_2(\nu)$ a meaningless exercise for values of ν greater than a few hundred MeV. We will return to the question of measuring $f_2(\nu)$ in the final section, and turn our attention now to the evaluation of the dispersion relation for $f_1(\nu)$, which, with the low energy theorem value for $f_1(0)$ now reads

$$\operatorname{Re} f_1(\nu) = -\frac{\alpha}{M_N} + \frac{\nu^2}{\pi} P \int_{\nu_0}^{\infty} \frac{d\nu'^2}{\nu'^2 - \nu^2} \frac{\operatorname{Im} f_1(\nu')}{\nu'^2}$$

or   (14)

$$\operatorname{Re} f_1(\nu) = -\frac{\alpha}{M_N} + \frac{\nu^2}{2\pi^2} P \int_{\nu_0}^{\infty} \frac{d\nu'}{\nu'^2 - \nu^2} \sigma_T(\nu') .$$

III. FITS TO THE TOTAL PHOTOABSORPTION CROSS SECTIONS

In order to carry out the principal value integral in Eq. (14) we need the total cross section measurements[10,11,12,13,14] shown in Figure 1. In fact, we need them in a locally smoothed form in order to carry out the limiting procedure inherent in the definition of a principal value integral, and furthermore, at least in principle, we need to know the cross sections out to infinite values of the energy.

At least this last difficulty is not difficult to overcome if we are willing to assume that at high energies the behavior of total cross sections with energy is smooth (say, a sum of powers of ν to good approximation). In particular, this is the case in Regge pole theory where at high energies one writes for the imaginary

part of the amplitude at $t = 0$:

$$\mathrm{Im}\, f_1(\nu) = \sum_i \left(\frac{c_i}{4\pi}\right) \nu^{\alpha_i(0)} , \tag{15}$$

so that

$$\sigma_T(\nu) = \sum_i c_i \nu^{\alpha_i(0)-1} , \tag{16}$$

where the c_i are constants and the $\alpha_i(0)$ are the $t = 0$ intercepts of the Regge trajectories, $\alpha_i(t)$, which can be exchanged in the t-channel. Such parametrizations give very good fits to the energy dependence of purely hadronic total cross sections (like $\pi^\pm p$, $K^\pm p$, etc.). There it is found that the leading isospin $= 0$ and 1 trajectories (those with $\alpha_i(0) > 0$) are the Pomeron (corresponding to diffraction scattering and constant total cross sections) which has $\alpha_P(0) = 1$ and the P', A_2, ρ and ω trajectories, all of which have $\alpha(0) \simeq 0.5$ as determined either from drawing the usual linear Regge trajectories (with slope $\approx 1/\mathrm{GeV}^2$) through the observed physical particle positions or from fits to the hadron-hadron total cross sections at high energies[15]. For Compton scattering only t-channel trajectories with $C = +1$ contribute, so we can restrict our attention here to only the P' and A_2 trajectories in addition to the Pomeron. We take $\alpha_P(0) = 1$ and the effective intercept at $t = 0$ of the P' and A_2 to be $\frac{1}{2}$, i.e.,
$\alpha_{P'}(0) = \alpha_{A_2}(0) = \frac{1}{2}$.

We have therefore made fits to the high energy data ($\nu > 2$ GeV) of the form:

$$\sigma_T(\nu) = c_1 + c_2/\nu^{\frac{1}{2}} . \tag{17}$$

In Figure 2 we see the high energy total cross section data from the extrapolation of electron scattering to $q^2 = 0$. They are plotted against $1/\nu^{\frac{1}{2}}$ so that if Eq. (17) is to be a good fit to the data points, they should fall on a straight line. In Figure 2 the solid line represents $\sigma_T(\nu) = 107.5 + 64.0/\nu^{\frac{1}{2}}$, which is a best fit statistically of the form of Eq. (17) to the data from the extrapolation of electron scattering. In Figure 3 we have the data from the direct measurements of the counter and bubble chamber experiments. The solid line is a best fit to these counter and bubble chamber experiments of the form $\sigma_T(\nu) = 99.2 + 59.6/\nu^{\frac{1}{2}}$. Also shown in Figures 2 and 3 is a dashed line, corresponding to a best fit to all the high energy data of the form $\sigma_T(\nu) = 96.6 + 70.2/\nu^{\frac{1}{2}}$.

It seems from the figures that the data from electron scattering is systematically and/or statistically high by about 8 μb compared to the other data, but has about the same slope as a function of energy. This is all well within the quoted[10] ± 8% overall systematic error alone of the electron scattering extrapolation. It is difficult to know, however, whether the "true" total cross sections should agree with one of the present set of measurements or another since each method of measurement has different kinds of systematic errors associated with it and an estimate of these errors is not always quoted in the experimental papers. For this reason we have kept three different fits of the form of Eq. (17) to the high energy ($\nu > 2$ GeV) total cross sections in doing the dispersion integral: a fit to the electron scattering extrapolation cross sections alone (labelled A), a fit to the counter and bubble chamber measurements alone (labelled B), and a fit to all the total cross section measurements (labelled A & B). If we were to show a prejudice for one fit over another it would be in favor of the fit (B) to the counter and bubble chamber measurements

which, when extrapolated to lower energies, joins on better to the total cross section measurements at the end of the resonance region coming from both the electron scattering extrapolation to $q^2 = 0$ and from the counter and bubble chamber measurements.

It is also to be noted that the size of the present experimental error bars does not permit one accurately to determine $\alpha(0)$ in a fit to the total photoabsorption cross sections of the form $\sigma_T(\nu) = c_1 + c_2 \, \nu^{\alpha(0)-1}$. While values of $\alpha(0)$ equal to zero or one are probably already ruled out by the present data, fits with values of $\alpha(0)$ ranging from 0.3 to 0.7 were tried and the resulting values of chi squared of the best fit for each value of $\alpha(0)$ were not significantly different. We thus have to rely on the much more accurate hadronic total cross section data to determine $\alpha(0)$. This is no great tragedy since: (1) the strong interaction data is accurate enough to show that in a fit of the form $\sigma_T(\nu) = c_1 + c_2 \, \nu^{\alpha(0)-1}$ that $0.3 \leq \alpha(0) \leq 0.7$ for the P' and A_2; (2) there is no reason to assume, in contradiction to Regge pole theory, that the value of $\alpha_{P'}(0)$ or $\alpha_{A_2}(0)$ changes in going from one process to another; (3) a fit of the form of Eq. (17) is an excellent fit to the photoproduction data, particularly the counter and bubble chamber data with small error bars in Figure 3. In any case, the exact value of $\alpha(0)$ makes little difference in the calculated values of $\mathrm{Re}\,f_1(\nu)$ at low energy and we shall return to the question of the sensitivity of the calculation at high energy to the value of $\alpha(0)$ in Section V.

Once we have a fit of the form of Eq. (17) to the high energy data, we use it to give us the total cross section over the entire high energy region for use in doing the dispersion integral. We also join on to it the data in the low energy region, which we take to be from threshold, $W = 1.08$ GeV ($\nu = 0.150$ GeV),

to a center of mass energy $W = 2.01$ GeV ($\nu = 1.68$ GeV), where the systematic measurements of $\sigma_T(\nu)$ in steps of 0.015 GeV in center of mass energy by the electron scattering group end. This includes the region of the four prominent resonances in pion-nucleon scattering at $W = 1.236$, 1.520, 1.690, and 1.920 GeV, respectively. To the total cross sections determined by extrapolation of electron scattering we have added the total cross section data up to $W = 1.32$ GeV obtained by integrating single pion photoproduction data[16].

We have then smoothed, again with the use of some physics: We fit this low energy data to a sum of Breit-Wigner resonance forms plus a polynomial background, demanding that at $W = 2.01$ GeV the fit join on smoothly to one of the high energy fits discussed above. Specifically, we used five Breit-Wigner resonance forms and a sixth order polynomial in $(W-W_{threshold})$ to obtain our best fits to the data. The masses of the first three resonance forms were only roughly constrained (to within $\pm$ 0.100 GeV) to lie in the vicinity of the prominent resonance bumps, and their widths were also only roughly constrained (to be less than 0.5 GeV). The fourth resonance was fixed with a mass and width of 1.920 and 0.200 GeV, respectively, since it otherwise had a tendency to wander to lower energies. The fits were improved if the fifth resonance mass was constrained to lie between 1.400 and 1.470 GeV, i.e., in the region of the Roper resonance, in order to fit the shoulder in the data on the low energy side of the second resonance. Otherwise all masses, widths and strengths of the resonances were left free to vary, as were all the coefficients in the polynomial in $W-W_{threshold}$.

The fit to the low energy data which joins on to $\sigma_T(\nu) = 96.6 + 70.2/\nu^{\frac{1}{2}}$, the best fit to all the high energy data, at $W = 2.01$ GeV (where $\sigma_T = 151$ μb) is

shown in Figure 4. Obviously we have a very good (as statistical tests also show) smooth fit to the total cross section data. Its stability is shown by the fact that changing the form of the high energy cross section from one of our fits to another (so that at W = 2.01 GeV, the energy at which we join the low energy to high energy cross sections, σ_T(W = 2.01 GeV) changes by $\sim$ 3% or $\sim$ 5 μb) does not change the fit by more than 1% at any point up to W = 1.95 GeV. The fit is stable as well against taking a lower degree polynomial to describe the background. Also the values of the resonance widths which come out of the fit are in good agreement with the accepted ones. Armed with our smooth fits to both the low and high energy total cross sections, we are ready to do the dispersion integral.

IV. CALCULATION OF THE REAL PART OF $f_1(\nu)$

For each of our three fits to the high energy data we have made a fit to the low energy data which joins on smoothly at W = 2.01 GeV, and then have used the total smoothed fit over the whole energy range from threshold to infinite energy as input to a computer calculation of the dispersion integral for $\mathrm{Re}\,f_1(\nu)$. We have tested our program for doing the principal value integrals by taking explicit forms for the total cross section for which we were capable of doing the principal value integral analytically and then comparing the analytic solution with the computer calculation. In particular

$$\frac{4\pi}{\nu}\,\mathrm{Im}\,f_1(\nu) = \sigma_T(\nu) = \left(\frac{\sigma\nu_0}{\nu}\right)\left(\frac{\nu^2}{\nu_0^2} - 1\right)^{\alpha/2} \quad \text{for } \nu \geq \nu_0$$

$$= 0 \quad \text{for } \nu < \nu_0 \,,$$

(18)

where σ is a constant leads to

$$\mathrm{Re}\, f_1(\nu) = f_1(0) + \frac{\nu_0 \sigma}{4\pi} \left[-\cot\left(\frac{\pi\alpha}{2}\right) \left(\frac{\nu^2}{\nu_0^2} - 1\right)^{\alpha/2} + \frac{1}{\sin\frac{\pi\alpha}{2}} \right] \tag{19a}$$

for $\nu > \nu_0$ and

$$\mathrm{Re}\, f_1(\nu) = f_1(0) + \frac{\nu_0 \sigma}{4\pi} \left[-\frac{1}{\sin\frac{\pi\alpha}{2}} \left(1 - \frac{\nu^2}{\nu_0^2}\right)^{\alpha/2} + \frac{1}{\sin\frac{\pi\alpha}{2}} \right] \tag{19b}$$

for $\nu < \nu_0$. For $\alpha = \frac{1}{2}$ we find that our program gives $\mathrm{Re}\, f_1(\nu)$ in agreement with the analytic solution to better than 1% accuracy from $\nu = 0$ to 50 GeV with the exception of a small region near threshold ($0.9\,\nu_0 \le \nu \le 1.1\,\nu_0$) where $df_1(\nu)/d\nu$ is discontinuous for the analytic solution and where the finite step size ($\approx 0.1\,\nu_0$) in our integration routine gives a computed real part which is 20% less than the exact analytic solution.

The actual results for $\mathrm{Re}\, f_1(W)$, computed from the fits to the measured total cross sections (where at high energies we use the fit (A & B) to all the high energy data of the form $\sigma_T(\nu) = 96.6 + 70.2/\nu^{\frac{1}{2}}$) is shown in Figure 5 for $W < 2.2$ GeV in the form of an Argand diagram. Clear circles due to the first, second, third and fourth resonances are seen. A close inspection also reveals a "wiggle" near $W = 1.430$ GeV due to the shoulder on the low energy side of the second resonance, which could be due to the Roper resonance. A similar, but smaller, wiggle appears near threshold due to the large s-wave shoulder on the low energy side of the first resonance. Using a different fit to the high energy total cross sections leaves Figure 5 essentially unchanged — the only noticeable change is in the size of the loop due to the fourth resonance

and involves changes in $\mathrm{Re}\, f_1(\nu)$ of less than 10% for any given value of ν. The numerical values of the input total cross sections, $\mathrm{Im}\, f_1(W)$, and the resulting values of $\mathrm{Re}\, f_1(W)$ appear in Table I in steps of 0.015 GeV in W up to W = 2.01 GeV, and then in steps of 1.0 GeV in ν up to $\nu = 20$ GeV.

Near $\nu = 0$, we have from the dispersion relation that

$$\lim_{\nu \to 0} \frac{f_1(\nu) - f_1(0)}{\nu^2} = \frac{1}{\pi} \int_{\nu_0}^{\infty} \frac{d\nu'^2}{\nu'^4} \, \mathrm{Im}\, f_1(\nu') = \frac{1}{2\pi^2} \int_{\nu_0}^{\infty} \frac{d\nu'}{\nu'^2} \, \sigma_T(\nu') \, . \tag{20}$$

From our fit to the data we find

$$\frac{1}{2\pi^2} \int_{\nu_0}^{\infty} \frac{d\nu'}{\nu'^2} \, \sigma_T(\nu') = 72 \, \mu b/\mathrm{GeV} \, , \tag{21}$$

with a 2% variation depending on exactly which combination of low and high energy data we use for the total cross section. Clearly the integral converges quickly and its magnitude depends very weakly on the high energy data. Near $\nu = 0$ we thus have for forward photon-proton scattering:

$$\left(\frac{d\sigma}{d\Omega_{\mathrm{lab}}} \right)_{\theta = 0^\circ} = |\, f_1(\nu)\,|^2 + |\, f_2(\nu)\,|^2$$

$$\xrightarrow[\nu \to 0]{} \left(\frac{\alpha}{M_N} \right)^2 \left[1 + \frac{\nu}{m_\pi}^2 \left(\frac{m_\pi^2 (\mu_{\mathrm{anom}})^4}{4 M_N^2} - \frac{M_N m_\pi^2}{\alpha \pi^2} \int_{\nu_0}^{\infty} \frac{d\nu'}{\nu'^2} \sigma_T(\nu') \right) + 0(\nu^4) \right]$$

$$\xrightarrow[\nu \to 0]{} \left(\frac{\alpha}{M_N} \right)^2 \left[1 - 0.88 \left(\frac{\nu}{m_\pi} \right)^2 + 0(\nu^4) \right] . \tag{22}$$

At high energies calculated values of $\mathrm{Re}\, f_1(\nu)$ are shown by the solid lines in Figure 6 for the three cases of high energy fits to $\sigma_T(\nu)$ of the form:

$$\sigma_T(\nu) = 107.5 + 64.0/\nu^{\frac{1}{2}} \qquad \text{(labelled A) ;} \qquad\qquad (23a)$$

$$\sigma_T(\nu) = 99.2 + 59.6/\nu^{\frac{1}{2}} \qquad \text{(labelled B) ;} \qquad\qquad (23b)$$

$$\sigma_T(\nu) = 96.6 + 70.2/\nu^{\frac{1}{2}} \qquad \text{(labelled A \& B) .} \qquad\qquad (23c)$$

In addition, the ratio of real to imaginary parts at high energies is shown in Figure 7. Also shown in Figure 6 by the dashed lines are the real parts we might have naively expected on the basis of the imaginary part of the amplitude (the total cross sections) and Regge behavior for the whole amplitude. In other words, if we have that

$$\frac{4\pi}{\nu} \operatorname{Im} f_1(\nu) = \sigma_T(\nu) \rightarrow \sum_i c_i \nu^{\alpha_i(0)-1} \qquad \text{as } \nu \rightarrow \infty ,$$

we expect that such an $\operatorname{Im} f_1(\nu)$ came from a Regge expression for the full amplitude of the form:

$$f_1(\nu) \xrightarrow[\nu \rightarrow \infty]{} \sum_i \left(\frac{-1 - e^{-i\pi\alpha_i(0)}}{\sin \pi\alpha_i(0)} \right) \left(\frac{c_i}{4\pi} \right) \nu^{\alpha_i(0)} , \qquad\qquad (24)$$

where we have simply restored the signature factors due to the exchange of even signature (P, P' and A_2) trajectories. Thus we expect:

$$\operatorname{Re} f_1(\nu) \xrightarrow[\nu \rightarrow \infty]{} \sum_i \left(-\cot \frac{\pi\alpha_i(0)}{2} \right) \left(\frac{c_i}{4\pi} \right) \nu^{\alpha_i(0)} . \qquad\qquad (25)$$

For our particular fits, which are of the form $\sigma_T(\nu) \rightarrow c_1 + c_2/\nu^{\frac{1}{2}}$, we then expect that

$$\text{Re}\,f_1(\nu) \rightarrow -\left(\frac{c_2}{4\pi}\right)\nu^{\frac{1}{2}}, \tag{26}$$

which is represented by the dashed lines in Figure 6 for each of our high energy fits. For our high energy fits of the form (17) this is clearly not the case, there being always a constant difference of about $-3\ \mu$b-GeV between the real part calculated from the dispersion relation and the real part in Eq. (26) which is predicted naively from Regge theory and the behavior of the imaginary part of the amplitude. That we should have expected (as in actuality we did) such a constant difference between the calculated real part and the real part predicted from Regge theory and the high energy behavior of the imaginary part of the amplitude is shown in the next section.

V.   ASYMPTOTIC BEHAVIOR OF $\text{Re}\,f_1(\nu)$

Suppose we have an amplitude $f(\nu)$ which has the high energy behavior

$$f(\nu) \rightarrow \sum_{i,\ \alpha_i(0) > 0} \frac{-1 - e^{-i\pi\alpha_i(0)}}{\sin\pi\alpha_i(0)} \left(\frac{c_i}{4\pi}\right) \nu^{\alpha_i(0)} \tag{27}$$

$$+ C + \text{(terms which go to zero as } \nu \rightarrow \infty)\,,$$

where we have explicitly separated the term C (which is a real constant) which corresponds to a term in the sum with $\alpha_i(0) = 0$. The behavior of the real and imaginary parts following from Eq. (27) is

$$\text{Re}\, f(\nu) = \sum_{i,\, \alpha_i(0) \geq 0} \left(\frac{c_i}{4\pi}\right) \left(-\cot\left(\frac{\pi\alpha_i(0)}{2}\right)\right) \nu^{\alpha_i(0)}$$

$$+ \, C + (\text{terms which go to zero at } \nu \to \infty) , \tag{28a}$$

$$\text{Im}\, f(\nu) = \sum_{i,\, \alpha_i(0) > 0} \left(\frac{c_i}{4\pi}\right) \nu^{\alpha_i(0)}$$

$$+ \, (\text{terms which go to zero as } \nu \to \infty) . \tag{28b}$$

Now let us define $f^{(R)}(\nu)$ for all ν as:

$$f^{(R)}(\nu) = \sum_{i,\, \alpha_i(0) > 0} \frac{-1 - e^{-i\pi\alpha_i(0)}}{\sin\pi\alpha_i(0)} \left(\frac{c_i}{4\pi}\right) \nu^{\alpha_i(0)} + C . \tag{29}$$

Clearly, $f^{(R)}(\nu)$ differs from $f(\nu)$ only in terms which go to zero as $\nu \to \infty$. This new function obeys the dispersion relation

$$f^{(R)}(\nu) = C + \frac{\nu^2}{\pi} \int_0^\infty \frac{d\nu'^2}{\nu'^2 - \nu^2 - i\epsilon} \frac{\text{Im}\, f^{(R)}(\nu')}{\nu'^2} , \tag{30}$$

as is easily verified by explicit calculation, while it is assumed that the original amplitude $f(\nu)$ obeys a dispersion relation of the form:

$$f(\nu) = f(0) + \frac{\nu^2}{\pi} \int_{\nu_0}^\infty \frac{d\nu'^2}{\nu'^2 - \nu^2 - i\epsilon} \frac{\text{Im}\, f(\nu')}{\nu'^2} . \tag{31}$$

Now, from the way in which $f^{(R)}(\nu)$ was defined and Eq. (27) we have that

$$f(\nu) - f^{(R)}(\nu) \to 0 \quad \text{as } \nu \to \infty .$$

Subtracting Eq. (30) from Eq. (31), and letting $\nu \to \infty$, we then obtain

$$0 = f(0) - \frac{1}{\pi} \int_{\nu_0}^{\infty} \frac{d\nu'^2}{\nu'^2} \operatorname{Im} f(\nu') - C + \frac{1}{\pi} \int_{0}^{\infty} \frac{d\nu'^2}{\nu'^2} \operatorname{Im} f^{(R)}(\nu') , \tag{32}$$

or

$$C = f(0) + \frac{1}{\pi} \int_{0}^{\nu_0} \frac{d\nu'^2}{\nu'^2} \operatorname{Im} f^{(R)}(\nu') + \int_{\nu_0}^{\infty} \frac{d\nu'^2}{\nu'^2} \operatorname{Im} \left(f^{(R)}(\nu) - f(\nu) \right) . \tag{33}$$

The last term in Eq. (33) involves a convergent integral because $f^{(R)}(\nu) - f(\nu)$ goes to zero is $\nu \to \infty$. In fact, in an actual calculation one usually assumes that for sufficiently large values of ν, say $\nu \ge N$, one has $\operatorname{Im} f(\nu) = \operatorname{Im} f^{(R)}(\nu)$ to arbitrarily high accuracy if N is chosen large enough. This is, of course, just what we have done in our calculation of $\operatorname{Re} f_1(\nu)$ when we used our Regge fits to the high energy total cross sections above $W = 2.01$ GeV in evaluating the dispersion relation. If we use the assumption that $\operatorname{Im} f^{(R)}(\nu) = \operatorname{Im} f(\nu)$ for $\nu \ge N$ in Eq. (33), then it becomes

$$C = f(0) + \frac{2}{\pi} \int_{0}^{N} \frac{d\nu'}{\nu'} \operatorname{Im} f^{(R)}(\nu') - \frac{2}{\pi} \int_{\nu_0}^{N} \frac{d\nu'}{\nu'} \operatorname{Im} f(\nu') \tag{34a}$$

or

$$\frac{1}{2\pi^2} \int_{\nu_0}^{N} d\nu' \, \sigma_T(\nu') = f(0) - C + \sum_i \left(\frac{c_i}{2\pi^2}\right) \frac{N^{\alpha_i(0)}}{\alpha_i(0)} \; , \qquad (34b)$$

so that it has the form of a finite energy sum rule[17]. Eq. (33) for the case $f(\nu) = f_1(\nu)$ was first derived in this form by Creutz, Drell and Paschos[18].

Eq. (33) or (34) tells us that purely from a knowledge of the imaginary part of $f(\nu)$ and $f(0)$, we can determine C, i.e., from the behavior of $\text{Im}\, f(\nu)$ at high energies we can determine $\text{Im}\, f^{(R)}(\nu)$ and then an integral over all energies of $\text{Im}(f(\nu) - f^{(R)}(\nu))$ gives us C if we know $f(0)$. All this of course should be no surprise — given the imaginary part of $f(\nu)$ and $f(0)$, the dispersion relation gives us $\text{Re}\, f(\nu)$ and we can then determine the constant C by comparison with $\text{Re}\, f^{(R)}(\nu)$. This in fact is just what we did in the last section. What all the above manipulation does for us is to bypass the actual calculation of the principal value integral and to give us a simple sum rule, Eq. (34), from which we can calculate C immediately by doing an ordinary integral over total cross sections.

For the particular amplitude we are interested in, we have $f_1(0) = -\alpha/M_N = -3.0 \; \mu$b-GeV. Furthermore, from the measured total cross sections we see that above $W \approx 2$ GeV $\text{Im}\, f_1(\nu)$ appears to be rather smooth. This is also the point at which systematic measurements in small steps of W stop at the present time and at which we have joined the power law fits to the high energy data onto the low energy data in doing our calculation of the dispersion integral. We are thus <u>assuming</u> that above $W = 2.01$ GeV the power law fits are a good representation of the total cross sections, i.e., above $W = 2.01$ GeV ($\nu = 1.68$ GeV) we are assuming $\text{Im}\, f(\nu) - \text{Im}\, f^{(R)}(\nu) = 0$. The sum rule, Eq. (34), thus becomes:

$$C = -\frac{\alpha}{M_N} + \frac{2}{\pi} \int_0^{(1.68\,\text{GeV})} \frac{d\nu'}{\nu'} \operatorname{Im} f_1^{(R)}(\nu') - \frac{2}{\pi} \int_{\nu_0}^{(1.68\,\text{GeV})} \frac{d\nu'}{\nu'} \operatorname{Im} f_1(\nu') . \qquad (35)$$

For the quantity,

$$-\frac{\alpha}{M_N} - \frac{2}{\pi} \int_{\nu_0}^{(1.68\,\text{GeV})} \frac{d\nu'}{\nu'} \operatorname{Im} f_1(\nu') ,$$

which just involves performing an integral over the total cross section data, we obtain $-19.9 \pm 0.1\,\mu$b. The "error" includes the answers obtained by taking different computer smoothed fits to the low energy data (which join onto different high energy behaviors), taking the unsmoothed data, or taking hand smoothed fits to the data. The value of

$$\frac{2}{\pi} \int_0^{(1.68\,\text{GeV})} \frac{d\nu'}{\nu'} \operatorname{Im} f_1^{(R)}(\nu')$$

depends on exactly what kind of power law fit we make to which subset of the high energy data. We list the parameters for fits to the high energy data subsets A, B, and A & B of the form $\sigma_T(\nu) = c_1 + c_2(\nu/\text{GeV})^{\alpha(0)-1}$ for $\alpha(0) = 0.6$, 0.5, and 0.4 in Table II, together with the values of $\frac{2}{\pi} \int_0^{1.68\,\text{GeV}} (\frac{d\nu'}{\nu'}) \operatorname{Im} f_1^{(R)}(\nu')$ and C which they imply.

From Table II it appears that (at least if $\alpha(0) \gtrsim 0.5$) C $\simeq -3\,\mu$b-GeV, i.e., it has the magnitude and sign of the Thomson limit, $f_1(0)$, a possibility first suggested by Creutz, Drell and Paschos[18]. For the case $\alpha(0) = \frac{1}{2}$, the values of C computed in Table II agree with those found in the previous section (see Figure 6) by direct computation of $\operatorname{Re} f_1(\nu)$ and comparison with the real part expected from Regge theory and the behavior of $\operatorname{Im} f_1(\nu)$ at high energies.

The errors contained in such a calculation of C are mainly of a systematic kind and hence difficult to estimate. The integral over the low energy total cross section measurements, $\frac{2}{\pi} \int_{\nu_0}^{1.68\,\text{GeV}} (\frac{d\nu'}{\nu'})\, \text{Im}\, f_1(\nu')$, involves over 60 data points with an assigned error of about 10%. If these were purely statistical errors, the error on the value of the integral would be $\sim 1\%$. Similarly, given a value of $\alpha(0)$, the errors in c_1 and c_2 in the fit to the high energy total cross sections (induced from the quoted errors on σ_T) lead to an uncertainty in $\frac{2}{\pi} \int_{0}^{1.68\,\text{GeV}} (\frac{d\nu'}{\nu'})\, \text{Im}\, f_1^{(R)}(\nu')$ of from 5% (for fits to data set B) to 10% (for fits to data set A).

To change the value of C from $-3\,\mu\text{b-GeV}$ to zero requires a 20% change in one or the other (or some combination) of the two integrals discussed above. For the integral over the low energy total cross sections this can only happen due to a systematic overall shift (downward) from the present data. We think such a large systematic shift is unlikely because the total cross sections obtained from the extrapolation of electron scattering agree rather well in the first resonance region with those obtained by directly integrating over single pion photoproduction differential cross sections.

A change in the value of the integral over the Regge fit to the data could come about either because of a systematic shift (upward, particularly at the low energy end, in order to give more energy dependence to $\sigma_T(\nu)$) in the high energy total cross section measurements or a value of $\alpha(0) \approx 0.4$. A systematic shift in the high energy data certainly cannot be ruled out, but such a shift upwards would be difficult to reconcile with a smooth joining on to the low energy data, particularly if one also wants to help decrease the magnitude of C by a systematic shift downward in that same low energy data. It should

also be noted that the fits (B) to only the counter and bubble chamber experiments at high energies, which have the smallest quoted errors, give the largest magnitude for C. As for the value of $\alpha(0)$, which is representing here the effective Regge trajectory intercept of the P' and A_2, we note first of all that the most important of these two trajectories for the case at hand appears[19] to be the P'. Secondly, the best fits to the hadronic data of the form $\sigma_T = c_1 + c_2 \nu^{\alpha(0)-1}$, especially recent fits[20] using both finite energy sum rules and the hadronic total cross section data, show that $\alpha_{P'}(0) \simeq 0.5$ or greater, not smaller.

Thus, while the possibility exists that a combination of systematic shifts in the data and/or a change in Regge parameters will result in making C consistent in magnitude with zero[21], it is suggested by the present data and our high energy Regge fits to it that $C \neq 0$, and in fact that $C \simeq -3$ μb-GeV, the value of the Thomson limit. In Regge language, such a real constant term in the high energy forward amplitude could correspond to a Regge pole with $\alpha(0) = 0$. Whether $\alpha(t) \equiv 0$, so that we are dealing with a fixed pole at $J = 0$, can only be established by calculations for $t \neq 0$, which are outside the scope of this paper. In any case, the presence of such an extra real constant term at $t = 0$ already has some interesting consequences theoretically for other calculations and sum rules[22].

VI. CONCLUSION

Under the assumption that the forward dispersion relation for $f_1(\nu)$ of Gell-Mann, Goldberger and Thirring is correct we have calculated $\operatorname{Re} f_1(\nu)$ from the measurements of the total photoabsorption cross section. In the process we have made smooth fits to both the low and high energy cross sections. Our results suggest, but do not conclusively prove, the existence of an extra real constant in the high energy behavior of $f_1(\nu)$ beyond what the energy dependence of the imaginary part and Regge theory would predict.[18] This extra real constant is consistent in sign and magnitude with the value of the Thomson limit, $f_1(0) = -\alpha/M_N$.

There are a number of experiments which could help settle the question of whether the extra real constant, C, is present. Obviously more accurate total photoabsorption cross sections even at the energies already measured will help. More important are systematic counter or bubble chamber measurements in the energy range from $\nu = 1.0$ to 3.0 GeV. These are needed first of all to make sure that the cross sections in the upper resonance region, which come at present only from the electron scattering extrapolation, are not systematically high or low. Secondly, such measurements will show whether above $\nu = 1.68$ GeV (where we have joined on our high energy fits) the total cross section has any small "bumps" left in it and more generally how well our smooth fit to the high energy data fits the total cross sections just above the resonance region. Some total cross section measurements of high accuracy at the other end of the energy spectrum, namely very high energies (say, $\nu = 30$ to 150 GeV at Serpukhov or Weston) would be very useful in tying down the other end of our high energy fits.

Between these two additional sets of measurements we think one can settle the
question of whether $C \neq 0$ and whether it has the value of the Thomson limit to
within 50% of that limit.

Of course, all this could be best settled by a good direct measure-
ment of $\mathrm{Re}\, f_1(\nu)$. This would also test the validity of the forward dispersion
relation, which we have been assuming in our discussion of the magnitude of C.
At $\nu = 5$ GeV, for example, the presence of $C = f_1(0)$ makes a 20% difference
in the value of $\mathrm{Re}\, f_1(\nu)$. Unfortunately, it does not appear that we will soon have
such a measurement. Recall that $(d\sigma/dt)_{t=0} \propto |\, f_1(\nu)\,|^2 + |\, f_2(\nu)\,|^2$ for Compton
scattering. Thus the forthcoming measurements of $(d\sigma/dt)_{t=0}$ will give us
$|\, \mathrm{Re}\, f_1(\nu)\,|^2 + |\, f_2(\nu)\,|^2$, since we know $\mathrm{Im}\, f_1(\nu)$ from the total cross section
measurements. Since we find $|\, \mathrm{Re}\, f_1/\mathrm{Im}\, f_1\,| \lesssim 0.3$ for $\nu > 5$ GeV, $|\, \mathrm{Re}\, f_1(\nu)\,|^2$
contributes less than 10% of $(d\sigma/dt)_{t=0}$ for $\nu > 5$ GeV. This is of the same order
as the error in $|\, \mathrm{Im}\, f_1(\nu)\,|^2$ due to the errors in the total cross section mea-
surements, so the measurement of $(d\sigma/dt)_{t=0}$ at high energy will only yield a
very rough upper bound[23] on $|\, \mathrm{Re}\, f_1(\nu)\,|$. At the present time it is probably more
relevant to assume the forward dispersion relations are true and then to derive
information from $(d\sigma/dt)_{t=0}$ about $|\, f_2(\nu)\,|^2$ at high energy, since experimentally
we know essentially nothing at present about the high energy behavior of $f_2(\nu)$.[24]

This leaves us with trying to measure $\mathrm{Re}\, f_1(\nu)$ at low energies where
it is large compared to $\mathrm{Im}\, f_1(\nu)$. Because of background from $\pi^0 \to 2\gamma$ it is ex-
tremely difficult to measure $(d\sigma/dt)_{t=0}$ for Compton scattering at low energies.
Our best hope of testing the dispersion relation is then the possibility of mea-
suring $\mathrm{Re}\, f_1(\nu)$ by interference of the amplitude for electron-positron production
by Compton scattering with the Bethe-Heitler amplitude[5], and then extrapolating

to zero invariant mass electron-positron pairs. Exactly how difficult this will prove to be experimentally remains to be seen.

A side result of our calculation is that the ratio of real to imaginary parts of the forward Compton amplitude is much the same as that for most strong interaction forward amplitudes[25]. In particular, if we omit the contribution of the possible extra real constant, then the ratio of real to imaginary parts is less than 20% above $\nu \approx 5$ GeV, much as in pion-nucleon scattering (even keeping the real constant, the ratio is less than 30%). If we assume the validity of the vector dominance model, then the forward amplitude for $\gamma + p \rightarrow \rho + p$ should have a similar ratio of real to imaginary parts. The recently suggested[26] ratio of -0.45 at 6 GeV is then much too large compared to our calculation or to other strong interaction processes.

So, although the prospects still do not look very good for an early experimental test of the forward dispersion relations, we have seen a number of interesting consequences of our study of forward Compton scattering. In particular, we hope that we have provided sufficient encouragement to experimentalists to make further measurements of the total photoabsorption cross sections, to measure the magnitude of $(d\sigma/dt)_{t=0}$ for Compton scattering, and to try to measure $\text{Re} f_1(\nu)$ by interference of the Bethe-Heitler amplitude with the Compton amplitude for pair production.

ACKNOWLEDGEMENTS

REFERENCES

1. M. Gell-Mann, M. L. Goldberger, and W. Thirring, Phys. Rev. $\underline{95}$, 1612 (1954).

2. See, for example, the rapporteur talks by M. L. Goldberger and S. Mandelstam in The Quantum Theory of Fields, Proceedings of the Twelfth Solvay Conference, Brussels, Belgium, 1961 (Interscience Publishers, New York, 1961), pp. 179-196 and 209-224.

3. H. Anderson et al., Phys. Rev. $\underline{100}$, 339 (1955). See also the more recent comparison in the resonance region in pion-nucleon charge exchange by W. Risk, Phys. Rev. $\underline{167}$, 1249 (1967), and references therein.

4. K. J. Foley et al., Phys. Rev. Letters $\underline{19}$, 143 (1967); ibid $\underline{19}$, 857 (1967).

5. S. J. Brodsky et al., Phys. Rev. (in press).

6. M. Gell-Mann and M. L. Goldberger, Phys. Rev. $\underline{96}$, 1433 (1954). F. Low, Phys. Rev. $\underline{96}$, 1428 (1954).

7. We shall use a notation where $\alpha = e^2/4\pi = 1/137$. All energies are in GeV, with $M_N = 0.94$ GeV, $m_\pi = 0.14$ GeV in all numerical computations.

8. S. D. Drell and A. C. Hearn, Phys. Rev. Letters $\underline{16}$, 908 (1966); S. B. Gerasimov, Sov. J. Nucl. Phys. $\underline{2}$, 430 (1966).

9. Y. C. Chau, N. Dombey, and R. G. Moorhouse, Proceedings of the 1967 International Symposium on Electron and Photon Interactions at High Energies, SLAC, Stanford, California, 1967, p. 617; G. C. Fox and D. Z. Freedman, Phys. Rev. $\underline{182}$, 1628 (1969). It should be noted that although the sum rules for the proton or neutron separately appear to be satisfied, their difference (which involves an isoscalar-isovector photon interference) does not appear to be satisfied according to Fox and Freedman.

10. E. D. Bloom et al., SLAC-PUB-653, 1969 (unpublished).

11. D. O. Caldwell et al., University of California at Santa Barbara preprint, 1969 (unpublished); and D. O. Caldwell, private communication.

12. H. Meyer et al., DESY preprints, 1969 (unpublished).

13. J. Ballam et al., Phys. Rev. Letters 21, 1544 (1968).

14. J. Ballam et al., Phys. Rev. Letters 23, 498 (1969).

15. See, for example, the review by V. Barger in Proceedings of the CERN Topical Conference on High Energy Collisions of Hadrons, Geneva, 1968, CERN 68-7, Vol. 1, p. 3.

16. R. T. Beale, S. D. Eklund, and R. L. Walker, California Institute of Technology Synchrotron Laboratory Report CTSL-42, 1966, unpublished. In the region of the first resonance the total cross sections obtained from extrapolation of inelastic ep scattering to $q^2 = 0$ (Ref. 10) agree quite well with these single pion cross sections, which are a little higher below resonance and a little lower above resonance.

17. R. Dolen, D. Horn, and C. Schmid, Phys. Rev. 166, 1768 (1968).

18. M. J. Creutz, S. D. Drell and E. A. Paschos, Phys. Rev. 178, 2300 (1969).

19. See the data on $\sigma_T(\gamma p) - \sigma_T(\gamma n)$ of Refs. 11 and 12 and the talk by H. Harari presented at the Fourth International Symposium on Electron and Photon Interactions at High Energies, Liverpool, England, September 1969. From the data it appears that the A_2 contribution to the decreasing part of the total cross section is less than 30% of the P' contribution.

20. See V. Barger and R. J. N. Phillips, Wisconsin preprint, 1969 (unpublished). We thank Professor Barger for a discussion of this work and other determinations of $\alpha_{P'}(0)$.

21.   We thank M. Creutz at SLAC and M. Wong at DESY for discussions on their work and the possible errors in calculations of the value of C.

22.   See the discussion of the neutron-proton mass difference in the talk of F. J. Gilman presented at the <u>Fourth International Symposium on Electron and Photon Interactions at High Energies,</u> Liverpool, England, September, 1969. Sum rules for forward Compton scattering on $I = 1$ targets (with $I = 2$ in the t-channel) could also be effected by a similar fixed pole at $J = 0$. We thank H. Harari for discussions on this subject.

23.   See in this connection J. K. Walker, Phys. Rev. Letters <u>21</u>, 1618 (1968).

24.   The energy dependence of $f_2(\nu)$ is interesting from the point of view of Regge theory since it receives a leading contribution from trajectories of even signature and odd parity which is otherwise hidden by higher trajectories. See the discussion in S. L. Adler and R. F. Dashen, <u>Current Algebras</u> (W. A. Benjamin, New York, 1968), p. 330.

25.   See V. Barger, Ref. 15. Our ratio of $\mathrm{Re}\, f_1/\mathrm{Im}\, f_1$ also appears to be in rough agreement with that found in a dispersion relation calculation done at DESY with somewhat different initial input: see J. Weber, DESY internal report, DESY F1-69/3, July 1969.

26.   J. Swartz and R. Talman, Phys. Rev. Letters <u>23</u>, 1078 (1969). Conversely, if it is shown experimentally that the ratio of real to imaginary parts of the forward amplitude for $\gamma + p \to \rho + p$ is -0.45, then the calculated ratio of real to imaginary parts for the forward Compton amplitude, which is much smaller in magnitude, would mean the vector dominance model connection between the two processes breaks down.

TABLE I

Calculated values of $\mathrm{Re}\, f_1(\nu)$ for forward photon-proton scattering.
The input values of $\sigma_T(\nu) = \frac{4\pi}{\nu}\, \mathrm{Im}\, f_1(\nu)$ (from the smooth fit at low energy which
joins on to the fit (A & B) to all the high energy data) as well as the resulting
values of $\mathrm{Re}\, f_1(\nu) - \mathrm{Re}\, f_1(0)$ and $\mathrm{Re}\, f_1(\nu)$ are listed in steps of 0.015 GeV in W
up to W = 2.01 GeV, and then in steps of 1.0 GeV in ν up to ν = 20 GeV.

W (GeV)	ν (GeV)	$\sigma_T(\nu)$ (μb)	$\mathrm{Im}\, f_1(\nu)$ (μb-GeV)	$\mathrm{Re}\, f_1(\nu)-\mathrm{Re}\, f_1(0)$ (μb-GeV)	$\mathrm{Re}\, f_1(\nu)$ (μb-GeV)
.945	0.005	0	0.0	+ 0.0018	− 3.0
.960	0.020	0	0.0	0.030	− 3.0
.975	0.036	0	0.0	0.094	− 2.9
.990	0.051	0	0.0	0.20	− 2.8
1.005	0.067	0	0.0	0.35	− 2.7
1.020	0.083	0	0.0	0.55	− 2.5
1.035	0.100	0	0.0	0.82	− 2.2
1.050	0.116	0	0.0	1.2	− 1.8
1.065	0.133	0	0.0	1.7	− 1.3
1.080	0.150	0	0.0	2.7	− 0.3
1.095	0.168	75	1.0	3.7	+ 0.7
1.110	0.185	114	1.7	4.0	+ 1.0
1.125	0.203	145	2.3	4.5	+ 1.5
1.140	0.221	182	3.2	5.3	+ 2.3
1.155	0.240	233	4.4	6.2	+ 3.2
1.170	0.258	307	6.3	7.0	+ 4.0
1.185	0.277	404	8.9	7.1	+ 4.1
1.200	0.296	499	11.8	5.6	+ 2.6
1.215	0.315	546	13.7	2.4	− 0.6
1.230	0.335	522	13.9	− 1.3	− 4.3
1.245	0.354	449	12.7	− 4.1	− 7.1
1.260	0.374	366	10.9	− 5.4	− 8.4
1.275	0.395	292	9.2	− 5.7	− 8.7
1.290	0.415	235	7.8	− 5.2	− 8.2

W (GeV)	ν (GeV)	$\sigma_T(\nu)$ (μb)	$\mathrm{Im}\,f_1(\nu)$ (μb–GeV)	$\mathrm{Re}\,f_1(\nu)-\mathrm{Re}\,f_1(0)$ (μb–GeV)	$\mathrm{Re}\,f_1(\nu)$ (μb–GeV)
1.305	0.436	196	6.8	− 4.3	− 7.3
1.320	0.457	172	6.3	− 3.1	− 6.1
1.335	0.478	162	6.2	− 1.9	− 4.9
1.350	0.499	164	6.5	− 0.7	− 3.7
1.365	0.521	175	7.2	+ 0.3	− 2.7
1.380	0.543	190	8.2	+ 0.9	− 2.1
1.395	0.565	207	9.3	+ 1.2	− 1.8
1.410	0.587	220	10.3	+ 1.1	− 1.9
1.425	0.610	228	11.1	+ 0.9	− 2.1
1.440	0.633	234	11.8	+ 0.8	− 2.2
1.455	0.656	241	12.6	+ 1.0	− 2.0
1.470	0.679	253	13.7	+ 1.1	− 1.9
1.485	0.703	271	15.2	+ 0.8	− 2.2
1.500	0.727	288	16.6	− 0.5	− 3.5
1.515	0.751	290	17.3	− 2.5	− 5.5
1.530	0.775	275	17.0	− 4.3	− 7.3
1.545	0.800	255	16.2	− 5.1	− 8.1
1.560	0.824	239	15.6	− 5.2	− 8.2
1.575	0.849	228	15.4	− 4.9	− 7.9
1.590	0.875	222	15.4	− 4.7	− 7.7
1.605	0.900	219	15.7	− 4.5	− 7.5
1.620	0.926	218	16.1	− 4.3	− 7.3
1.635	0.952	219	16.6	− 4.3	− 7.3
1.650	0.978	221	17.2	− 4.2	− 7.2
1.665	1.005	225	18.0	− 4.3	− 7.3
1.680	1.031	232	19.1	− 4.7	− 7.7
1.695	1.058	239	20.2	− 6.1	− 9.1
1.710	1.085	236	20.3	− 8.2	− 11.2
1.725	1.11	219	19.4	− 9.8	− 12.8
1.740	1.14	201	18.3	− 10.3	− 13.3
1.755	1.17	187	17.4	− 10.1	− 13.1
1.770	1.20	176	16.8	− 9.8	− 12.8
1.785	1.22	168	16.4	− 9.3	− 12.3
1.800	1.25	163	16.2	− 8.8	− 11.8
1.815	1.28	159	16.2	− 8.2	− 11.2
1.830	1.31	158	16.5	− 7.6	− 10.6
1.845	1.34	158	16.9	− 7.0	− 10.0
1.860	1.37	161	17.5	− 6.6	− 9.6
1.875	1.40	164	18.3	− 6.5	− 9.5
1.890	1.43	167	19.0	− 6.6	− 9.6
1.905	1.46	170	19.7	− 7.0	− 10.0
1.920	1.49	170	20.2	− 7.6	− 10.6
1.935	1.52	168	20.4	− 8.2	− 11.2
1.950	1.55	165	20.3	− 8.7	− 11.7
1.965	1.58	160	20.2	− 9.0	− 12.0
1.980	1.62	156	20.1	− 8.9	− 11.9
1.995	1.65	153	20.0	− 8.8	− 11.8
2.010	1.68	151	20.2	− 8.5	− 11.5

W (GeV)	ν (GeV)	$\sigma_T(\nu)$ (μb)	$\mathrm{Im}\,f_1(\nu)$ (μb–GeV)	$\mathrm{Re}\,f_1(\nu)-\mathrm{Re}\,f_1(0)$ (μb–GeV)	$\mathrm{Re}\,f_1(\nu)$ (μb–GeV)
2.16	2.0	146	23.4	– 8.3	– 11.2
2.55	3.0	137	32.6	– 9.6	– 12.5
2.90	4.0	132	41.9	– 11.0	– 13.9
3.21	5.0	128	51.0	– 12.3	– 15.2
3.49	6.0	125	60.0	– 13.4	– 16.3
3.75	7.0	123	68.7	– 14.5	– 17.3
3.99	8.0	121	77.3	– 15.5	– 18.3
4.22	9.0	120	86.0	– 16.5	– 19.3
4.44	10.0	119	94.6	– 17.4	– 20.2
4.64	11.0	118	103	– 18.3	– 21.1
4.84	12.0	117	112	– 19.1	– 21.9
5.03	13.0	116	120	– 19.9	– 22.7
5.22	14.0	115	129	– 20.7	– 23.5
5.39	15.0	115	137	– 21.5	– 24.3
5.56	16.0	114	145	– 22.2	– 25.0
5.73	17.0	114	154	– 22.8	– 25.6
5.89	18.0	113	162	– 23.5	– 26.2
6.05	19.0	113	170	– 24.1	– 26.8
6.20	20.0	112	179	– 24.8	– 27.5

TABLE II

Parameters for fits to the high energy total cross section measurements of the form $\sigma_T(\nu) = c_1 + c_2(\nu/\text{GeV})^{\alpha(0)-1}$, corresponding values of $\frac{2}{\pi}\int_0^{(1.68\text{ GeV})}\frac{d\nu'}{\nu'}\text{Im}\,f_1^{(R)}(\nu')$, and resulting values of C taking

$$+\frac{\alpha}{M_N} + \frac{2}{\pi}\int_{\nu_0}^{(1.68\text{ GeV})}\frac{d\nu'}{\nu'}\text{Im}\,f_1(\nu') = 19.9\ \mu\text{b-GeV}.$$

Experimental Data Subset	$\alpha(0)$	c_1 (μb)	c_2 (μb)	$\frac{2}{\pi}\int_0^{(1.68\text{ GeV})}\frac{d\nu'}{\nu'}\text{Im}\,f_1^{(R)}(\nu')$ (μb-GeV)	C (μb-GeV)
A^{10}	0.6	100.5	68.1	16.4	− 3.5
$B^{11,12,13,14}$	0.6	93.5	61.7	15.1	− 4.8
A & B	0.6	89.9	72.9	16.1	− 3.8
A^{10}	0.5	107.5	64.0	17.5	− 2.4
$B^{11,12,13,14}$	0.5	99.2	59.6	16.2	− 3.7
A & B	0.5	96.6	70.2	17.4	− 2.5
A^{10}	0.4	112.2	62.5	19.2	− 0.7
$B^{11,12,13,14}$	0.4	102.9	59.9	18.1	− 1.8
A & B	0.4	101.2	70.1	19.5	− 0.4

FIGURE CAPTIONS

Figure 1 – The total photoabsorption cross section, $\sigma_T(\nu)$, for $\gamma + p \rightarrow$ hadrons measured in recent experiments.[10,11,12,13,14]

Figure 2 – High energy total photoabsorption cross sections[10] from the extrapolation of inelastic ep scattering to $q^2 = 0$ plotted versus $1/\nu^{\frac{1}{2}}$. The solid line is a best fit to these data of the form $\sigma_T(\nu) = c_1 + c_2/\nu^{\frac{1}{2}}$, with $c_1 = 107.5\ \mu b$, $c_2 = 64.0\ \mu b$, and ν measured in GeV. The dashed line is a similar fit to all the high energy data with $c_1 = 96.6\ \mu b$ and $c_2 = 70.2\ \mu b$.

Figure 3 – High energy total photoabsorption cross sections[11,12,13,14] from counter and bubble chamber measurements plotted versus $1/\nu^{\frac{1}{2}}$. The solid line is a best fit to these data of the form $\sigma_T = c_1 + c_2/\nu^{\frac{1}{2}}$ with $c_1 = 99.2\ \mu b$, $c_2 = 59.6\ \mu b$ and ν measured in GeV. The dashed line is a similar fit to all the high energy data with $c_1 = 96.6\ \mu b$ and $c_2 = 70.2\ \mu b$.

Figure 4 – Smooth fit (solid line) to the low energy total photoabsorption cross sections from extrapolation of inelastic ep scattering[10] to $q^2 = 0$ (data points shown in the figure) and from integrating single pion photo-production differential cross sections up to W = 1.32 GeV. Above W = 2.01 GeV the fit joins smoothly on to $\sigma_T(\nu) = 96.6 + 70.2/\nu^{\frac{1}{2}}$, the best fit to all the high energy data.

Figure 5 – Argand diagram of $f_1(W)$ for forward photon-proton scattering where $\mathrm{Re}\, f_1(W)$ was computed using the dispersion relation, Eq. (14). The input total cross sections are shown at low energy by the solid line in Figure 4 and at high energy by the dashed line in Figures 2 and 3.

Figure 6 –   Values of $\text{Re}\,f_1(\nu)$ at high energy calculated using the dispersion

relation, Eq. (14), are indicated by the solid lines for the three dif-

ferent fits (A, B, and A & B) to the high energy total cross sections

(see text). The real parts expected from Regge theory and the

observed behavior of the imaginary part of the amplitude are indi-

cated by the dashed lines for each of the three high energy fits.

Figure 7 –   Ratio of real to imaginary part of $f_1(\nu)$ at high energies calculated

using the dispersion relation, Eq. (14), for each of the fits to the

high energy total cross sections.

Fig. 1

Fig. 2

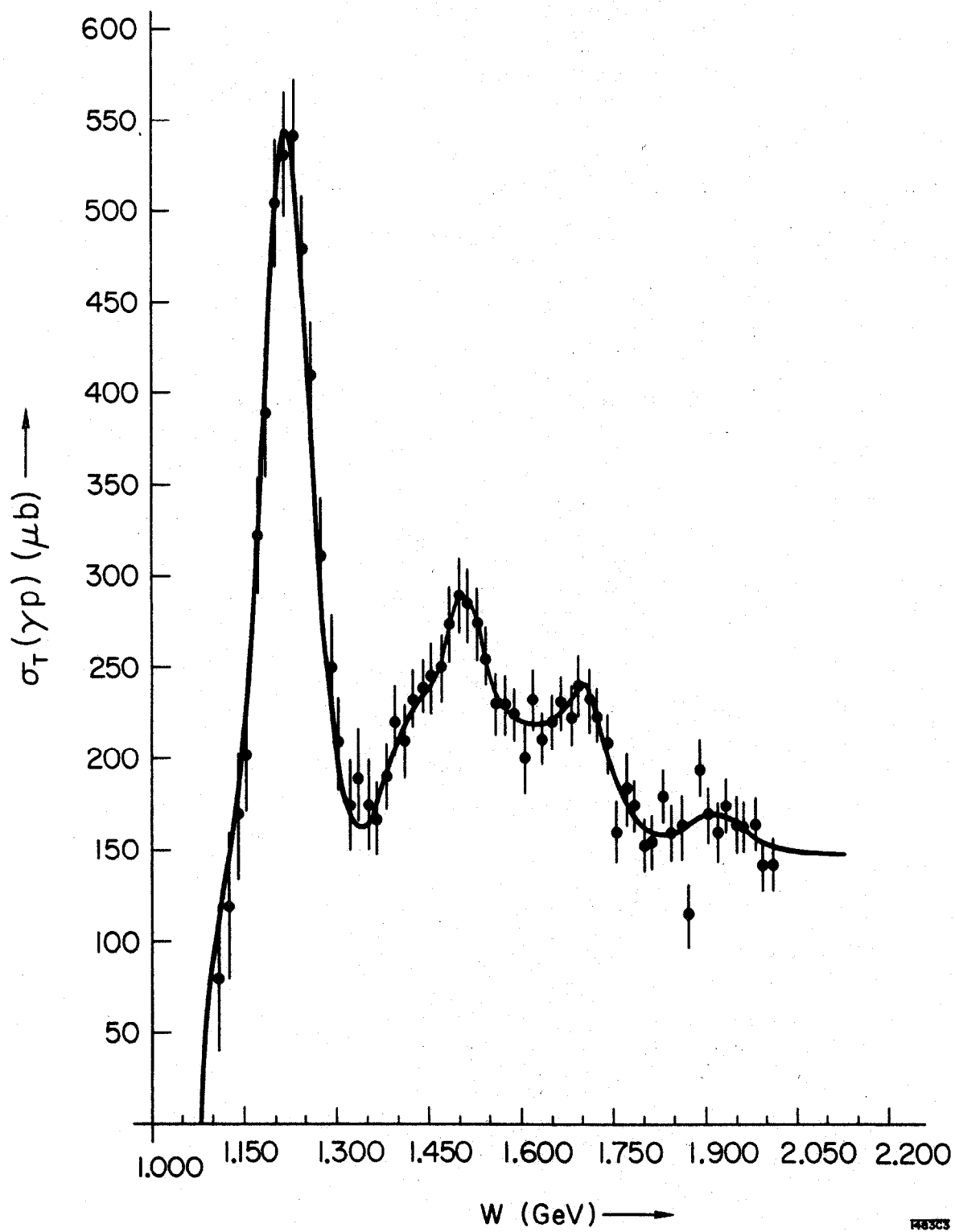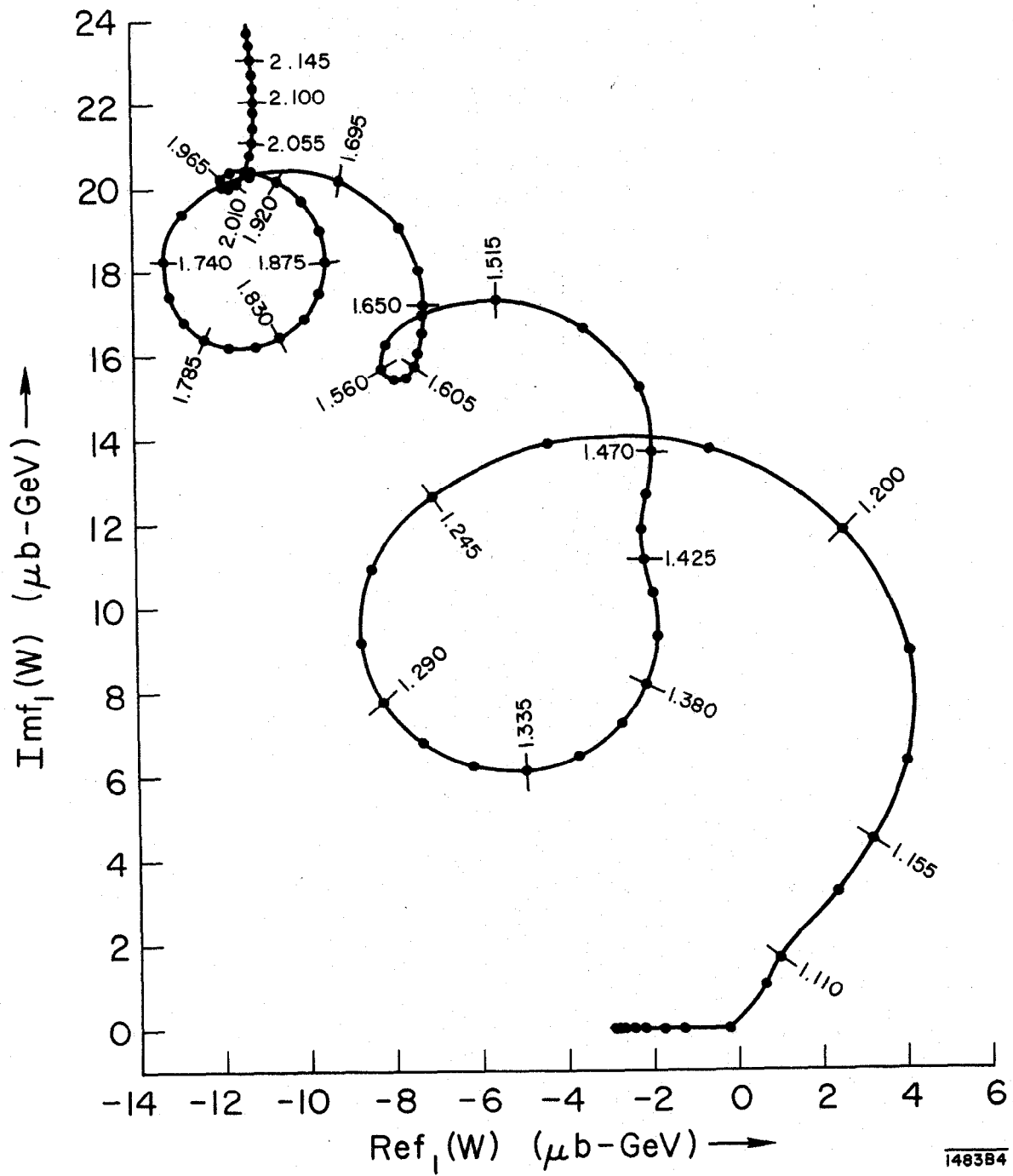Axis labels: $\sigma_T(\gamma p)$ (μb) (vertical), $1/(\nu/\text{GeV})^{\frac{1}{2}}$ (horizontal)

W = 2.0 GeV

1483BI

Fig. 3

Fig. 4

Fig. 5

Fig. 6

Fig. 7

148385